

Green processes for environmental application. Electrochemical ozone production*

L. M. Da Silva¹, L. A. De Faria², and J. F. C. Boodts^{1,2,‡}

¹Depto. de Química, FFCLRP/USP, Av. Bandeirantes, 3900. 14040-901. Ribeirão Preto - SP, Brazil; ²Instituto de Química, UFU, Campus Santa Mônica, Av. João Naves de Ávila, 2160. 38400-902, Uberlândia - MG, Brazil

Abstract: Several aspects of electrochemical ozone production (EOP) on β -PbO₂ were investigated. The morphology of the electrode material was determined *in situ* using extensive (total, external, and internal differential capacity) and intensive parameters (the morphology factor, φ) permitting comparison with results of other laboratories if appropriate electrode characterization parameters are available. The influence of the nature of the supporting electrolyte on the oxygen evolution reaction (OER)/EOP processes was investigated using polarization curves, recorded under quasi-stationary conditions, point-by-point polarization, and chronopotentiometry. The performance of the several β -PbO₂/electrolyte system was evaluated using the apparent specific power criterion. A detailed mechanism for EOP is proposed.

INTRODUCTION

Due to intense industrialization, actually, humans are faced with a number of serious problems such as: environment deterioration, global warming, energy, etc. Profound discussion of these issues is still at an initial stage, as several of the basic parameters governing these issues are not even well understood. However, all of the specialists involved in the discussion agree that steps must be taken to avoid further degradation of the planet. As a result, environmental legislation has become much more stringent causing a significant research effort in such areas as environmental monitoring and clean-up, CO₂ sequestration, new industrial processes (clean chemical processes) as well as the reevaluation of the older ones, etc.

Ozone being an environmentally clean reagent with proven efficiency for several processes of technological importance, a renewed interest in its production and application is observed [1–28]. Despite O₃ production via the corona process being rather expensive, the chemical has a number of appealing advantages: It is a very strong oxidant; its decomposition leads to environmentally friendly products (O₂); its instability ($t_{1/2} = 20\text{--}90$ min, depending on environment) requires that it is produced “on spot”, thereby reducing transportation and storage expenses. As a result, O₃ has found application in fields such as: water treatment, combustion of resistant organics, clean-up of effluents, bleaching of wood pulp [2,8,15,16,29].

An increasingly important O₃ application is its use as a disinfectant in purified water loops for the pharmaceutical and electronic industries, where extreme standards of purification [21,30] are needed. Ozone treatment, combined with UV-irradiation, flocculation, and biological treatment of heavily polluted effluents is very appealing. Traditionally, chlorine dioxide is a widely used and efficient bleaching agent of the wood pulp industry, causing, however, severe aggression to the environment [2,3]. The

*An issue of reviews and research papers based on presentations made at the IUPAC/ICSU Workshop on Electrochemistry and Interfacial Chemistry in Environmental Clean-up and Green Chemical Processes, Coimbra, Portugal, 6–7 April, 2001.

‡Corresponding author: jfcboodts@ufu.br

substitution of chlorine dioxide by O_3 as a bleaching agent permits the development of totally chlorine free (TCF) bleaching technology, reducing significantly the pollution burden and potential health hazard of chlorine derivatives of this industrial activity.

The traditional way to produce O_3 is the well-established corona technology, which is based on passing a electric discharge through dry oxygen or air. A promising alternative technology is electrochemical ozone production (EOP) from aqueous electrolytes using high current and potential [1,2,4–29]. According to Foller and Kelsall [27], development of EOP technology is of interest because of some well-identified problems with the conventional corona discharge process, the main problem being the low O_3 concentration obtained, limiting the viability of O_3 as an oxidant for many potential applications.

The drastic operation conditions required for EOP (high overpotential and acid-supporting electrolyte) put a high demand on the nature of the electrode material. As a result, up to now most of the investigations have centered on β - PbO_2 [2,4–29], a cheap electrode material presenting good electric conductivity, resistance to corrosion, and high overpotential for the oxygen evolution reaction (OER) [1], which is thermodynamically favored over the EOP. However, recently some investigations involving electrode materials such as DSA[®] coatings, boron-doped diamond films, and glassy carbon have been reported in the literature [14,20,27,28].

The high $E_{O_3}^o$ value, permitting the attack of numerous organics, makes ozone especially attractive for wastewater treatment. One of the drawbacks of *ex situ* use of ozone is that the electric energy input is not totally exploited. Amadelli *et al.* [29] recently proposed an elegant way to overcome this problem, combining anodically generated O_3 with H_2O_2 produced at an O_2 cathode (cathodic oxidation). To do so, these authors swapped the O_3/O_2 gas mixture produced at the anode into the cathodic compartment containing the pollutant. H_2O_2 decomposition results in OH^\bullet radicals that initiate degradation. Amadelli *et al.* [29], using *trans*-3,4-dihydrocinnamic acid as a model compound, showed this approach to give superior results over *ex situ* O_3 -degradation or direct oxidation.

A significant contribution to EOP technology was given by Stucki and coworkers [2,21]. These authors developed an electrochemical ozone generator that evolves ozone directly into a stream of relatively pure water from the back of a porous PbO_2 in contact with a solid polymer perfluorinated sulphonic acid membrane electrolyte. This approach drastically reduces anode wear by avoiding the low interfacial pH normally observed in cells having a conventional design, when operated at high current densities.

Fundamental investigations [4,5,16,19,22,23,25,27] have demonstrated that besides factors such as the nature of the electrode material, temperature (especially the temperature at the electrode/electrolyte interface), and applied current density, EOP efficiency strongly depends on the chemical nature of the supporting electrolyte. Fluoro-anions are particularly promising EOP promoters. An alternative approach, recently investigated, is the immobilization of certain O_3 promoters such as F^- and Fe^{2+} [11,24] directly in the β - PbO_2 film.

Representative efficiency for the EOP technology, depending on the current density employed, is in the 10–15% range. However, efficiencies of up to 40% are reported [4,27] on glassy carbon and β - PbO_2 , using the less-common supporting electrolytes HBF_4 (62 wt %) or HPF_6 (7.3 mol dm^{-3}).

The goal of this paper is to discuss some fundamental aspects of the EOP and present some new contributions to the field correlating the performance for EOP with the β - PbO_2 electrode morphology, prepared so as to present different real surface areas.

EXPERIMENTAL

Electrode preparation

β - PbO_2 electrodes were prepared by electrodeposition from $Pb(NO_3)_2$ solutions ($[Pb^{2+}] = 0.2$ mol dm^{-3} ; pH = 2; $T = 60$ °C), onto both faces of a steel microsphere blasted Ti-supports (10 × 5 × 0.12 mm), pre-

viously etched in hot oxalic acid (10%). β -PbO₂ coatings were deposited on top of an intermediate platinum interlayer obtained by electrodeposition at 30 mA cm⁻² ($t = 5$ min) from H₂PtCl₆ solution (0.002 mol dm⁻³). β -PbO₂ deposition was done at constant anodic current: $i = 5$ mA cm⁻² (*Electrode-I*) or 20 mA cm⁻² (*Electrode-II*) using a 40 min deposition time.

The electrodes were mounted in a glass tube and sealed with silicon glue. Fluka “purum p.a.” products were used throughout.

Cell

A three-compartment all-glass cell (0.2 dm³) was used throughout. Ohmic drop was minimized using a Luggin capillary approaching the working electrode from below while two heavily platinized platinum counter electrodes ensured uniformity of the current on the two opposite faces of the samples. Electrode potentials were read against the reversible hydrogen electrode (RHE) containing the basic supporting electrolyte (BSE) (3.0 mol dm⁻³ H₂SO₄) and was submerged directly in the supporting electrolyte investigated.

Techniques and equipment

Work done by Ho *et al.* [31] showed that Tafel curves recorded using freshly prepared β -PbO₂ electrodes became reproducible after about 30 min of polarization. Therefore, to ensure reproducibility of the kinetic data, freshly prepared electrodes were initially conditioned by polarization at a high overpotential for 30 min prior to taking measurements.

Kinetic data were obtained recording polarization curves under quasi-stationary conditions (1 mV s⁻¹) while ozone production was investigated by point-by-point polarization curves obtained under galvanostatic conditions (data were measured at least 10 min after polarization). The curves were recorded at different temperatures.

An AUTOLAB (Eco Chemie, The Netherlands) electrochemical system (GPES), model PGSTAT20, was used throughout. Temperature control was done by means of a model FC55A01 FTS cooling system.

Ozone concentration in the N₂ carrier gas was analyzed by UV absorption at 254 nm, using a 10-cm optical path gas cell. Absorbance was read after 10 min of polarization when stationary conditions were observed. Current efficiency data were calculated according to the following equation:

$$\chi_{\text{O}_3} / \% = [(Abs \cdot \Phi \cdot z \cdot F) / (\xi \cdot b \cdot i_T)] \cdot 100 \quad (1)$$

where: *Abs* = absorbance at 254 nm; Φ = flux of N₂ (dm³ s⁻¹); z = number of electrons ($n = 6$); ξ = ozone absorptivity at 254 nm (3024 cm⁻¹ mol⁻¹ dm³ [32]); b = optical path (10 cm); i_T = total current (EOP + OER) (ampere); χ_{O_3} = current efficiency for EOP (%); F = Faraday's constant (96485 C mol⁻¹).

Electrochemical studies were carried out using as basic supporting electrolyte a 3.0 mol.dm⁻³ H₂SO₄ solution in the absence or presence of different fluoro-anion species (0.03 mol dm⁻³ NaF and 0.10 mol dm⁻³ HBF₄). All standard solutions were prepared volumetrically using twice-distilled water with a final pass through a Millipore Milli – Q_{plus} apparatus.

RESULTS AND DISCUSSION

In situ surface characterization of electrode before EOP

In situ characterization was done measuring the influence of the sweep rate, v , on the differential capacity following a procedure recently proposed [33]. Experimentally, 20 consecutive voltammetric curves are recorded, covering the 1.7–1.8 V/RHE capacitive potential interval. The total, C_T , and external, C_E , capacity values are obtained from the slopes of the straight lines in the i_c vs. v plots, respectively

observed in the low and high v -domains. To ensure the capacitive current obeys $i_c \cong C_d \cdot v$, current data should be measured from the voltammetric curves at a potential close to $E_{\lambda,a}$. Finally, the internal capacity, C_I , is calculated using next relation: $C_I = C_T - C_E$ (for more details, see ref. 33).

Table 1 shows the influence of the electrode preparation parameters on the internal, C_I , external, C_E , and total, C_T , differential capacities and the morphology factor, ϕ ($= C_I/C_T$). These parameters enable an evaluation of the real electrode surface and establish a base for comparison with data obtained by other groups.

Comparing the influence of the current density on the coating compactness, the data presented in Table 1 show that at the lower current density, used in the preparation of Electrode-I, a layer with a much lower real surface area (more compact) is obtained. The ϕ -values, however, are little affected by the current density, revealing that the internal, less accessible, regions of the films maintain about the same percentual contribution to the total surface area.

It is clear from the data of Table 1 that the more internal microstructure of the film (see C_I -values) represents the main contribution to the total surface area of the electrode, suggesting its electrochemical response will be important. However, one must keep in mind that these data are obtained under drastically different experimental conditions (capacitive potential region) from data secured in a potential region where a Faradaic process occurs. This experimental difference in securing capacity data is especially important in the case of gas-evolving electrode processes (EOP, OER) where clogging of the film microstructure by gas bubbles is a real possibility, thus reducing significantly the effective electrochemically active surface area.

Table 1 Surface parameters as function of electrode preparation.

β -PbO ₂ Electrode	C_T mF cm ⁻²	C_E mF cm ⁻²	C_I mF cm ⁻²	ϕ
I	58	15	43	0.74
II	100	22	78	0.78

Voltammetric behavior of β -PbO₂ electrodes in acid medium

Figure 1 shows a representative cyclic voltammogram, CV, of a β -PbO₂ electrode in 3.0 mol dm⁻³ H₂SO₄, together with the identification of relevant standard potentials (OER and EOP) and the start of

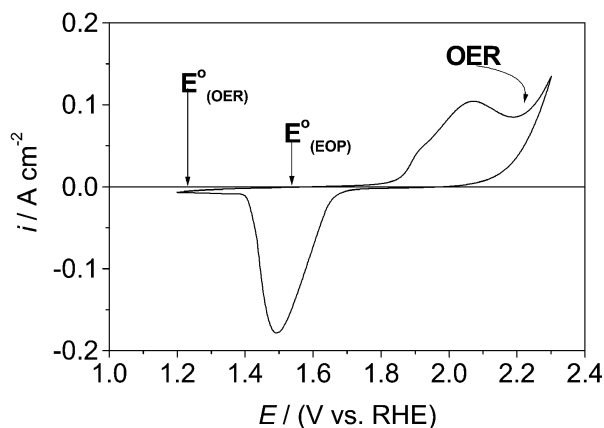


Fig. 1 Cyclic voltammogram of β -PbO₂ (Electrode-I) in 3.0 mol dm⁻³ H₂SO₄. $v = 20$ mV s⁻¹. $T = 24$ °C. Arrows indicate the thermodynamic standard potentials (E°) and the experimental potential where the oxygen evolution reaction, OER, initiates. EOP: electrochemical ozone production.

the OER. The voltammetric profile is characterized by a pair of peaks localized at 1.5 ($E_{p,a}$) and 1.2 ($E_{p,c}$) V (vs. RHE), which are attributed to the solid-state surface redox transitions (SSSRT) involving Pb(II)/Pb(IV) [34,35]. The anodic and cathodic voltammetric charges, q_a and q_c , respectively, obtained by integration of the voltammetric peaks furnishes q_a/q_c -values close to one showing the surface electrochemical processes to behave reversibly.

An important feature of Fig. 1 is the high overpotential (~ 1.0 V) displayed by β -PbO₂ for the OER attending one of the desirable requirements of any electrode material for EOP application, or be it, a potential electrode material must present a high overpotential for the OER, which is thermodynamically favored over EOP.

Kinetics: Influence of temperature and supporting electrolyte on OER/EOP

Oxygen evolution always occurs simultaneously with ozone formation. The presence at the electrode surface of different O-intermediates during EOP was proven by Wabner and Grambow for PbO₂ and Pt [36]. In any electrode mechanism proposed, the O₃-formation step is considered fast only depending on a well-succeeded encounter between atomic (O[•]) and molecular oxygen (O₂).

Figure 2 shows representative Tafel curves, already corrected for ohmic drop, iR , recorded under conditions of quasi-stationary potential sweep, for different SEs and temperatures.

Initially, it is worthwhile to emphasize that the profile of the Tafel curve in the high overpotential domain strongly depends on the procedure used (positive feedback or current interruption) to compensate for ohmic drop, as clearly demonstrated by Kötzt and Stucki [22] and Babak *et al.* [23]. In this paper, the iR correction procedure, initially proposed by Shub and Reznik [37] and successfully applied by us to several different metallic conductive electrode materials [38–40], was used. Experimental Tafel profiles corrected for iR by the Shub and Reznik procedure result very similar to the data obtained by the current interruption technique.

Independently of the supporting electrolyte used, R -values ($= R_{\Omega} + R_{\text{film}}$) are in the 0.12–0.26 Ω range, in excellent agreement with data obtained for other electrode materials having metallic conductance ($\rho_{\text{PbO}_2} = 0.95 \times 10^{-4} \Omega \text{ cm}$ [31]) submerged in an electrolyte showing good conductance.

After iR correction of the experimental data, Tafel curves were obtained (see Fig. 2) showing two linear segments proving the deviation from linearity observed in the experimental data is due to ohmic resistance combined with a change in the electronic transfer coefficient, α [41].

Figure 3 shows Tafel coefficients, obtained in the low and high overpotential domains for several temperatures located in the 0–30 °C interval, and different SEs, are dependent on these parameters.

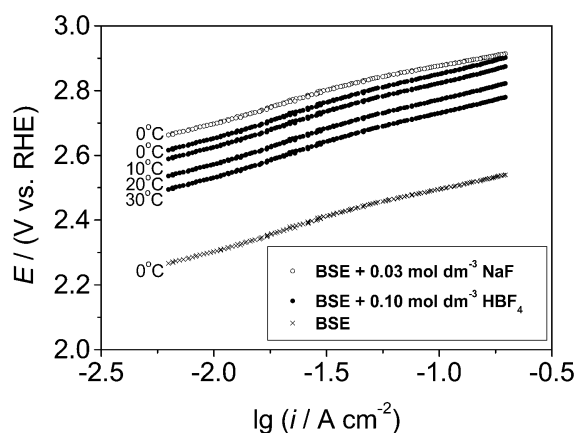


Fig. 2 Tafel curves as function of temperature (HBF₄) at 0 °C for the basic H₂SO₄ supporting electrolyte and in the presence of 0.03 mol dm⁻³ NaF or 0.10 mol dm⁻³ HBF₄.

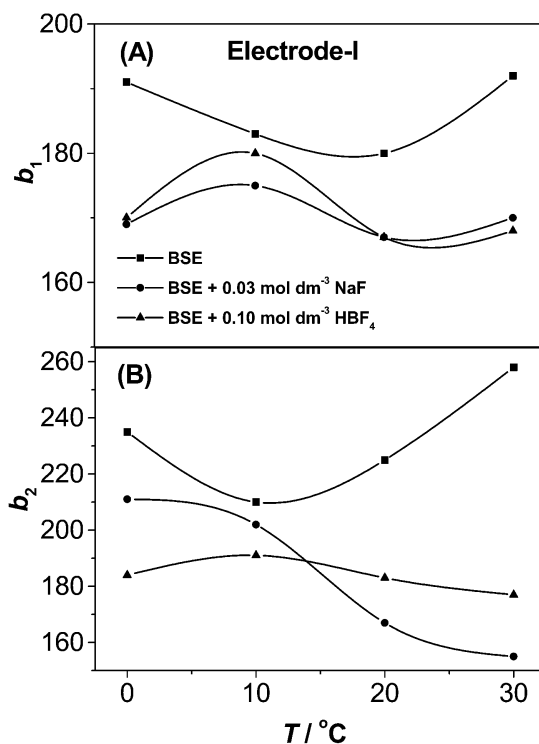


Fig. 3 Dependency of the Tafel coefficient, in the low (b_1) and high (b_2) current domains, on temperature for different supporting electrolytes. Electrode-I.

The numerical values are in good agreement with the results reported by Ho and Hwang [41] and support primary water discharge is the r.d.s.; the changes in b -values being attributed to changes in α . As can be seen from Figs. 2 and 3, OER and EOP kinetics, besides depending on the nature of the SE and temperature, also show the overpotential of these electrode processes increases in the presence of fluoro-anions.

With respect to temperature (see Fig. 3) a nonlinear dependence of the Tafel coefficient is experimentally obtained, contrary to theoretical prediction. This anomalous behavior of the Tafel coefficient with respect to temperature and the influence of the adsorption of electrolyte species (e.g., ions, dipoles, etc.) on solid electrode kinetics were investigated by Conway *et al.* [42] and Rüetschi [43]. Our results support the basic ideas of these authors and show that the kinetic behavior is governed by changes in the electronic behavior of the electrode surface (influence of anion adsorption on the electronic transfer coefficient) as well as partial blocking of the active surface sites by gas bubbles, as discussed by Ho and Hwang [41].

In the case of BSE, in the absence or presence of fluoro-species, adsorption of the sulphate anions and its displacement by the fluoro-species is a significant feature to be considered. Babak *et al.* [23] investigated the influence of the anions of the SE on the OER/EOP at PbO₂ in neutral pH media. These authors concluded that the changes in Tafel slope bear out a change in the mechanism that is involved with a different reactivity of the adsorbed intermediate. These conclusions are consistent with the results obtained under strong acidic conditions employed in this work.

Mechanistic proposal

Several electrode mechanisms to describe the OER/EOP, taking into account different intermediates, can be found in the literature [17,22,23,36]. However, none of these mechanisms considers the partial surface coverage of the several species involved in O₃-evolution.

O₃-evolution is represented by next global electrode mechanism:



Obviously, not all O₂ formed (the thermodynamically favored process) leads to O₃. In fact, O₃-formation strongly depends on the effective encounter of O₂ and O[•], which in turn depends on the partial surface coverage. We therefore propose the following detailed mechanism to describe the O₂/O₃ electrode processes

Mechanism for oxygen/ozone production	b/mV	
$(\text{H}_2\text{O})_{\text{ads}} \rightarrow (\text{OH}^\bullet)_{\text{ads}} + \text{H}^+ + \text{e}^-$	120	(3)
$(\text{OH}^\bullet)_{\text{ads}} \rightarrow (\text{O}^\bullet)_{\text{ads}} + \text{H}^+ + \text{e}^-$	40	(4)
$(\text{O}^\bullet)_{\text{ads}} \rightarrow [1-\theta](\text{O}^\bullet)_{\text{ads}} + \theta(\text{O}^\bullet)^*_{\text{ads}} \quad (\theta < \theta < 1)$		(5)
$[1-\theta](2\text{O}^\bullet)_{\text{ads}} \rightarrow [1-\theta](\text{O}_2)_{\text{ads}}$		(6)
$[1-\theta](\text{O}_2)_{\text{ads}} \rightarrow [1-\beta].[1-\theta](\text{O}_2)_{\text{ads}} + \beta[1-\theta](\text{O}_2)^*_{\text{ads}} \quad (\theta < \beta < 1)$		(7)
$[1-\beta].[1-\theta](\text{O}_2)_{\text{ads}} \rightarrow \text{O}_2 \uparrow$	15	(8)
$\theta(\text{O}^\bullet)^*_{\text{ads}} + \beta[1-\theta](\text{O}_2)^*_{\text{ads}} \rightarrow [\theta+\beta(1-\theta)](\text{O}_3)_{\text{ads}}$		(9)
$[\theta+\beta(1-\theta)](\text{O}_3)_{\text{ads}} \rightarrow \text{O}_3 \uparrow$	10	(10)

“θ” and “β” represent the surface coverage by oxygen species while “*” represents the fractional surface coverage leading to O₃.

In the above mechanism, EOP occurs at high overpotentials (current densities) via step 10 in parallel to step 8, the latter resulting in O₂-evolution. The high Tafel slopes ($b \geq 120$ mV) normally reported [16,17,25,31,41] for β-PbO₂ in strongly acid medium, support primary water discharge (step 3) is the r.d.s. controlling the electrode kinetics.

According to steps 8 and 10, partial current efficiencies with respect to the OER and EOP processes are governed by θ and β, as these parameters dependent on the phenomena occurring at the electrode/surface interface (e.g., bubble adherence, O[•] stability, etc.).

OER investigations at β-PbO₂ [41] from 1.0 mol dm⁻³ H₂SO₄ show O₂ bubble adherence at the electrode surface is an important factor controlling the kinetic behavior, as the Tafel slope is affected by both the electrocatalytic activity and the blockade of active sites. Additionally, the authors show that surface tension and buoyancy force of the adherent bubble is also affected by temperature.

Normally, OER/EOP investigations consider O₂ and O₃ the only electrolysis products [22], which is a reasonable assumption supported by Jordanis *et al.* [44] who showed that the formation of significant amounts of side-products can be excluded. However, as discussed recently by Amadelli *et al.* [25], at more anodic potentials, SO₄²⁻ can participate in Faradaic reactions yielding S₂O₈²⁻ [$E^\circ = 1.77$ or 1.88 V (vs. SCE)]. This process has been studied at several electrode materials (e.g., DSA-type, PbO₂, Pt) and is known to be favored in the presence of relatively high amounts of F⁻ [45–47].

Assuming the contribution of possible side reactions at elevated overpotentials is negligible, one can calculate, based on the electrode mechanism proposed above, the theoretical current efficiency for the OER/EOP processes as function of θ and β. Considering a unitary concentration for the total surface sites involved in the OER/EOP processes:

$$[\text{O}_2\text{-surface sites}] + [\text{O}_3\text{-surface sites}] = 1 \quad (11)$$

and considering the mechanism proposed:

$$[1-\beta].[1-\theta] + [\theta + \beta(1-\theta)] = 1 \quad (12)$$

Assuming the total Faradaic current is only due to the OER and EOP processes (no side reactions) the sum of the partial current efficiencies, χ_{O_2} and χ_{O_3} , respectively, can be written as:

$$\chi_{O_3} + \chi_{O_2} = 1 \quad (13)$$

and the theoretical current efficiency of the EOP process can be calculated from θ and β as:

$$\chi_{O_3} = [\theta + \beta \cdot (1 - \theta)] \quad (14)$$

Figure 4 shows the theoretical χ_{O_3} values for different θ and β -values, revealing optimum current efficiencies for EOP process are obtained for θ and β tending towards unity.

One of the important features of the simulation is that it clearly shows that experimental conditions optimizing the partial coverage factors θ and β result in a significant improvement of the O_3 current efficiency. So, a possible explanation for the significant improvement in χ_{O_3} observed in the presence of fluoro-anions is that these species provide in some way a more adequate effective surface coverage by the oxygen intermediates.

It is worthwhile to emphasize that in the case of β - PbO_2 the participation in the OER/EOP processes of a higher Pb oxidation state is not a reasonable proposal (Pb is already in its highest oxidation state), being more reasonable to consider β - PbO_2 as an “inert” surface.

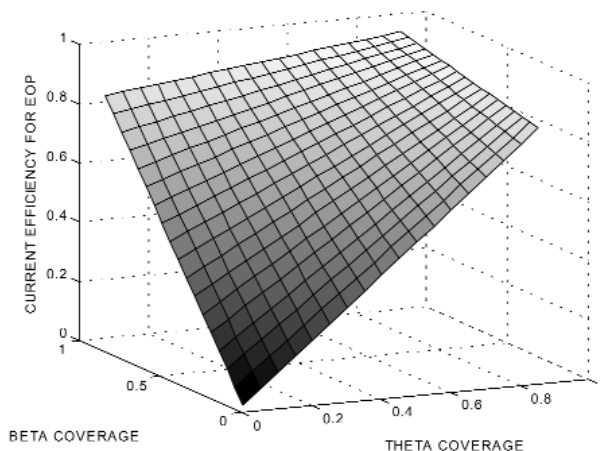


Fig. 4 Theoretical current efficiency for EOP as function of θ and β surface coverages.

Factors affecting the EOP process

Influence of the supporting electrolyte and electrode preparation on ozone production

Ozone current efficiencies strongly depend upon current density. Simply stated, one must increase the anode potential well beyond that of the oxygen evolution reaction for measurable ozone evolution to occur, and increasing current density is one of the most obvious means to accomplish this end. Thus, plots of ozone current efficiency vs. current density have been used frequently to characterize the reaction and the effects of other experimental parameters [26]. Several literature reports show the electrochemical activity of lead dioxide depends considerably on the composition of the electrolyte [25]. However, as mentioned earlier by Foller and Tobias [26], the literature on EOP reflects some confusion arising from a lack of understanding of the fundamental processes affecting current efficiency. Some discrepancy extends until nowadays as can be seen in different contributions found in the literature [17,22,24].

In particular, the nature of the electrolyte anions is known to have a marked influence on ozone and persulphate production. Thus, for example, an enhancement of these processes by F^- added to the

electrolyte is reported in the literature [23,25,48], while extreme values of approximately 40% current efficiency for the EOP process at different materials and reduced temperature were obtained using concentrated HBF_4 as SE [4,27].

Figure 5 shows the influence of current density and electrode preparation on χ_{O_3} , for different SEs, at 0 °C. With the exception of the BSE and BSE + F^- at Electrode-I, significant improvements in current efficiency are observed.

Once a minimum χ_{O_3} value is reached, apparently, gain in O_3 -production by further increasing the current density is only of minor importance. Apparently, what happens is that an equilibrium situation is reached, limited by bubble elimination from the surface, or-be-it, bubble residence time governs the process.

The influence of the electrode preparation parameters is a very interesting finding (see Fig. 5), especially the current density used to deposit the $\beta\text{-PbO}_2$ coating, on χ_{O_3} . Comparing the χ_{O_3} -values for the same SE at the two electrodes, with the exception of BSE where approximately the same χ_{O_3} -values are obtained, significant differences are observed in the presence of F^- and BF_4^- . Since for the BSE the current efficiency for O_3 -production is not significantly different at both electrodes, the morphologic effect observed in the presence of fluoro-anions cannot be explained by change in surface area of the two electrode (see Table 1). An even more intriguing result is the effect of BF_4^- which, using the H_2SO_4 supporting electrolyte as a reference, can act depending on electrode morphology as a promoter (Electrode-II) or inhibitor (Electrode-I) of the EOP process.

These findings are in agreement with the work of Chernik and coworkers [16] who showed that in the presence of F^- the anodic processes at $\beta\text{-PbO}_2$ are dependent on the surface state of the electrode material.

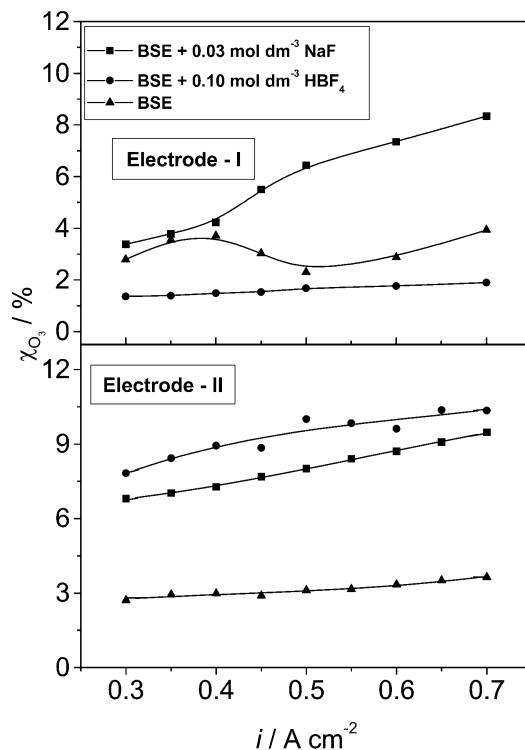


Fig. 5 Influence of current density on the ozone efficiency, χ_{O_3} , for different supporting electrolytes and electrode morphology (Electrodes I and II). $T = 0$ °C.

Influence of the temperature on EOP

As reported in the literature [4] the influence of the temperature on ozone yields is dependent on electrode material and nature of the supporting electrolyte. For example, as temperature is lowered in platinum anode electrolyses, ozone yields continue to improve even to the freezing points of eutectic compositions. On the contrary, in the case of PbO_2 anodes ozone yields at first improve and then decline as temperature is lowered.

Representative temperature vs. χ_{O_3} curves are shown in Fig. 6 for the BSE containing $0.10 \text{ mol dm}^{-3} \text{ HBF}_4$ at Electrode-II. One can observe that χ_{O_3} -values decrease with increasing temperature. This behavior is normally found in recent EOP investigations using temperature values $\geq 0^\circ \text{C}$ [17] and can be understood considering the increase in the anodic potential with decreasing temperature combined with a higher O_3 decomposition rate when the temperature is increased.

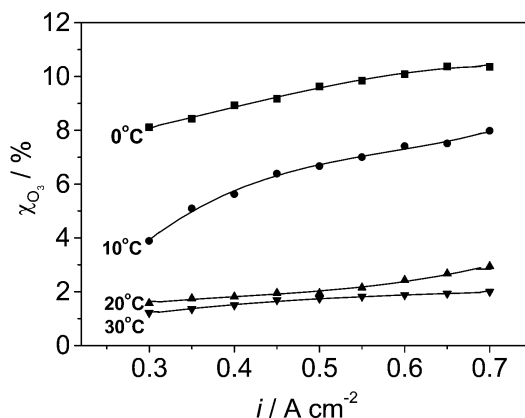


Fig. 6 Influence of temperature on the current efficiency for ozone production. Electrode-II; SE: BSE containing $0.10 \text{ mol dm}^{-3} \text{ HBF}_4$.

Analysis of the behavior of the polarization curves obtained point-by-point

Work done by Foller and Tobias [4] showed that during EOP anode potential, in galvanostatic polarization experiments, presents a time-dependent response. Therefore, electrolyses in this work were done by galvanostatic polarization using, after each current change, a 10 min waiting time to measure the potential. Figure 7 shows representative polarization curves, at 0°C , for the different SEs investigated. All potential values were corrected for ohmic drop using the R -values obtained in the kinetic investigation.

As shown in Fig. 7, the influence of the fluoro-anions on the E vs. i profiles reveals to be dependent on electrode morphology. While for the more compact coating (Electrode-I) the fluoro-anions cause an expressive effect on η over the complete current interval investigated, for the less compact coating (Electrode-II) the influence of the fluoro-anions is verified at $i \leq 0.3 \text{ A cm}^{-2}$.

While the behavior of the compact coating is in agreement with literature results [4,22,23], which normally report an increase in anode potential in the presence of fluoro-anions (e.g., F^-), the behavior observed with the less-compact coating (Electrode-II) was not reported in the literature. A comparison of the divergent behavior of Electrode-II with the normally reported behavior is difficult since EOP investigations at $\beta\text{-PbO}_2$ normally do not present information of the *in situ* characterization of the electrode material. Investigations under way in our laboratory, studying EOP at other electrode materials, also show that the presence of fluoro-anions only affects significantly the E vs. i profiles in the lower current domain ($i < 0.3 \text{ A cm}^{-2}$).

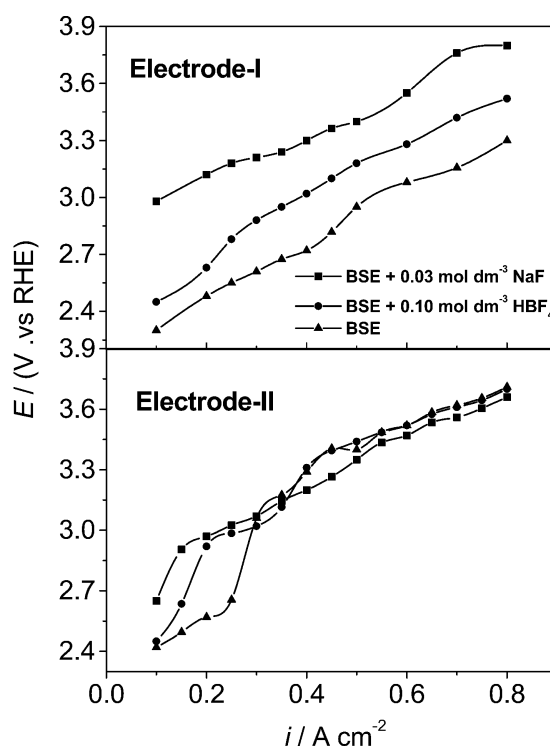


Fig. 7 Dependence of the E vs. i profiles on SE composition and electrode morphology. $T = 0$ °C.

Rationalization of the parameters involved in the potential-current density behavior surely points to such effect as: bubble adherence, anions, and dipoles adsorption—events which in turn are dependent on the rate of the electrode process, temperature, and hydrophobicity of the oxide surface.

A detailed investigation conducted by Foller and Tobias [4] analyzing the different factors governing EOP showed that, for a given SE, O_3 -production increases with increasing anode potential. This was also observed in this work up to a certain threshold potential above which increase in O_3 -production is only marginal. Comparing the different SEs, no direct correlation between the anodic potential (for a given current density) and χ_{O_3} was found.

Aiming at technological applications, the above results clearly establish a dependency between electrode morphology and χ_{O_3} , emphasizing the need for a detailed investigation of the electrode preparation parameters in order to optimize χ_{O_3} and reach a better understanding of the fundamental aspects involved.

Chronopotentiometric behavior in different supporting electrolytes

A chronopotentiometric investigation was executed to investigate the influence of the anion on the stabilization of the anode potential, E_a . Figure 8 shows representative E_a vs. t curves, corrected for ohmic drop, recorded at 0.95 A cm^{-2} and 0 °C.

In the case of the BSE and BSE-containing HBF_4 , E_a stabilizes rather rapidly contrary to the BSE-containing $0.03 \text{ mol dm}^{-3} \text{ NaF}$. For the later electrolyte, it takes ~ 10 min before E_a stabilizes, corroborating the time-dependent potential response observed by Foller and Tobias [4].

It is interesting to observe that for all SEs, after a state of equilibrium is reached, E_a stabilizes at about the same potential. Considering the extremely complex microstructure and its contribution (see

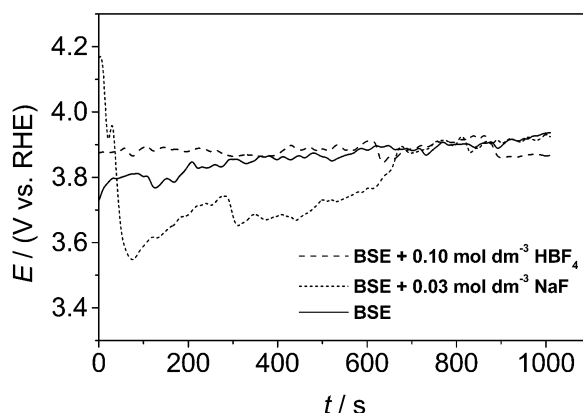


Fig. 8 Chronopotentiometric profiles as function of SE composition. Electrode-II; $T = 0\text{ }^{\circ}\text{C}$.

Table 1, C_T -values) to the overall electrode surface area, this result suggests that after equilibrium is reached the effective external surface area of the coating is about the same for all anions. The peculiar behavior of F^- suggests that initially ($t < 10\text{ min}$) the surface of the more internal electrode structure participates in the EOP process and is progressively excluded from the potential response.

Influence of the electrolyte on the apparent specific power consumption for EOP

According to the proposal of Stucki *et al.* [21], the efficiency of an electrochemical system for EOP can be evaluated using as a criterion the specific power for ozone, $P(\text{O}_3)^0$, expressed as Watt-hour per gram O_3 produced, following next expression:

$$P(\text{O}_3)^0 = (E \cdot z \cdot F) / (M \cdot \chi_{\text{O}_3}) \quad (15)$$

where: E = cell potential; z = number of electrons involved in the process ($z = 6$); F = Faraday's constant (96485 C mol^{-1}); M = molar mass (48 g mol^{-1}); χ_{O_3} = current efficiency for ozone. In eq. 15 the cell potential can be substituted by the anode potential, corrected for ohmic drop, resulting in the *apparent* specific power, useful to compare the influence of the SE on the efficiency of the system.

Table 2 presents $P(\text{O}_3)^0$ data as function of the SE and electrode morphology.

The $P(\text{O}_3)^0$ data show a dependency on both the supporting electrolyte and electrode morphology following next sequence: (i) Electrode-I: $P(\text{NaF}) < P(\text{H}_2\text{SO}_4) < P(\text{HBF}_4)$; (ii) Electrode-II: $P(\text{HBF}_4) \cong P(\text{NaF}) < P(\text{H}_2\text{SO}_4)$.

The $P(\text{HBF}_4)$ -data are consistent with the behavior observed in Fig. 5, showing this anion can act both as a promoter or inhibitor of EOP. The data also show the fluoro-anions give a superior efficiency in terms of energy involved in EOP while the observed dependency on electrode morphology once

Table 2 Dependence of apparent specific power, $P(\text{O}_3)^0$, for ozone as function of SE composition and electrode morphology. $i = 0.95\text{ A cm}^{-2}$; $T = 0\text{ }^{\circ}\text{C}$.

Electrolyte	H_2SO_4 3.0 mol dm^{-3}		NaF^a 0.03 mol dm^{-3}		HBF_4^a 0.10 mol dm^{-3}	
	I	II	I	II	I	II
$P(\text{O}_3)^0 / \text{Wh g}^{-1}$	310	331	116	142	360	132

^aBSE: $3.0\text{ mol dm}^{-3}\text{ H}_2\text{SO}_4$.

again emphasizes a need for complementary investigation aiming at the optimization of electrode preparation parameters.

Finally, when one is interested in evaluating the efficiency of a system for O₃-production, $P(\text{O}_3)^0$ is a more appropriate criterion than χ_{O_3} since the latter does not take into account the anode potential.

CONCLUSIONS AND PERSPECTIVES

The analysis of the literature reports together with the contribution presented in this paper show electrochemical ozone production is a promising alternative to corona technology, especially when high O₃-concentrations are required to viabilize certain applications. Electrochemical technology easily reaches current efficiencies above 15%.

A number of fundamental aspects are not yet totally understood, requiring further systematic investigation. Issues such as the role of anion adsorption, influence of bubble residence time apparently limiting ozone efficiency, hydrophobicity of the oxide surface, and electrode materials promoting better efficient contact between the oxygen intermediates leading to O₃-formation, all require further attention.

As shown in this paper, several electrochemical parameters of EOP on $\beta\text{-PbO}_2$ show an electrode morphology dependent response requiring electrode preparation parameters should be further investigated to optimize O₃-production, even at the well-known $\beta\text{-PbO}_2$ electrode.

Investigations of new electrode materials, having a higher overpotential for the OER, are highly desirable. However, with respect to this issue due to the high overpotential at which EOP occurs and high acidity of the coating/solution interface, stringent demands are put on the material in terms of wear.

Supporting electrolytes containing fluoro-anions surely improve the efficiency of the electrode process for O₃-production, including reducing energy consumption, a fundamental issue in electrochemical technology. However, much less research has been dedicated to supporting electrolytes others than fluoro-anions.

Some papers dealing with cell technology have appeared in the literature. Cell technology to cope with huge volumes (effluent treatment) or bulk processes (e.g., wood pulp bleaching) is required.

The detailed mechanism for EOP proposed in this paper permits a correlation between the steps involved in O₃-synthesis and the current efficiency, emphasizing surface stability of (O₂)_{ads} and (O[•])_{ads} is of fundamental importance to improve O₃-efficiency.

ACKNOWLEDGMENTS

L. M. Da Silva wishes to thank the Ph.D. Fellowship received from the FAPESP Foundation. J. F. C. Boodts and L. A. De Faria wish to thank financial support received from the CAPES/FAPEMIG/CNPq Foundations. J. F. C. Boodts acknowledges a Visiting Researcher Fellowship granted by the CNPq.

REFERENCES

1. R. G. Rice and A. Netzer (Eds.). *Handbook of Ozone Technology and Applications*, Vol. 1, Ann Arbor Science, England (1982).
2. S. Stucki, G. Theis, R. Kötze, H. Devantay, H. Christen. *J. Electrochem. Soc.* **132**, 367 (1985).
3. M. X. Meng and J. S. Hsieh. *Tappi J.* **83**, 67 (2000).
4. P. C. Foller and W. Tobias. *J. Electrochem. Soc.* **129**, 506 (1982).
5. P. C. Foller and M. L. Goodwin. *Ozone Science Eng.* **6**, 29 (1984).
6. K. Ota, H. Kaida, N. Kamiya. *Denki Kagaku Oyobi Kogyo Butsuri Kagaku* **55**, 465 (1987).
7. V. A. Shepelin, A. A. Babak, G. F. Potatova, E. V. Kasatkin, Yu. E. Roginskaya. *Elektrokhimiya* **26**, 1142 (1990).
8. T. C. Wen and C. C. Chang. *J. Chin. Inst. Chem. Eng.* **23**, 397 (1992).

9. P. Tatapudi and J. M. Pallav. *J. Electrochem. Soc.* **140**, 3527 (1993).
10. T. C. Wen and C. C. Chang. *J. Electrochem. Soc.* **140**, 2764 (1993).
11. J. Feng, D.C. Johnson, S. N. Lowery, J. J. Carey. *J. Electrochem. Soc.* **141**, 2708 (1994).
12. G. F. Potapova, E. V. Kasatkin, V. P. Nikitin, O. V. Shestakova, A. V. Blinov, A. F. Mazanko, A. I. Sorokin, S. A. Asaturov. *Bashk. Khim. Zh.* **2**, 65 (1995).
13. Y. Zhou, B. Wu, R. Gao, H. Zhang, W. Jiang. *Yingyong Huaxue* **13**, 95 (1996).
14. A. Perret, W. Haenni, P. Niedermann, N. Skinner, Ch. Comminellis, D. Gandi. *Proc. Electrochem. Soc.* 97 (1997).
15. J. K. Kim and B. S. Choi. *Hwahak Konghak* **35**, 218 (1997).
16. A. A. Chernik, V. B. Drozdovich, I. M. Zharskii. *Russ. J. Electrochem.* **33**, 259 (1997).
17. A. A. Chernik, V. B. Drozdovich, I. M. Zharskii. *Russ. J. Electrochem.* **33**, 264 (1997).
18. V. N. Fateev, S. V. Akel'kina, A. B. Velichenko, D. V. Girenko. *Russ. J. Electrochem.* **34**, 815 (1998).
19. A.A. Babak, R. Amadelli, V.N. Fateev. *Russ. J. Electrochem.* **34**, 149 (1998).
20. N. Katsuki, E. Takahashi, M. Toyoda, T. Kurosu, M. Lida, S. Wakita, Y. Nishiki, T. Shimamune. *J. Electrochem. Soc.* **145**, 2358 (1998).
21. S. Stucki, H. Baumann, H. J. Christen, R. Kötz. *J. Appl. Electrochem.* **17**, 773 (1987).
22. E. R. Kötz and S. Stucki. *J. Electroanal. Chem.* **228**, 407 (1987).
23. A. A. Babak, R. Amadelli, A. De Battisti, V. N. Fateev. *Electrochim. Acta* **39**, 1597 (1994).
24. A. B. Velichenko, D. V. Girenko, S. V. Kovalyov, A. N. Gnatenko, R. Amadelli, F. I. Danilov. *J. Electroanal. Chem.* **454**, 203 (1998).
25. R. Amadelli, L. Armelao, A. B. Velichenko, N. V. Nikolenko, D. V. Girenko, S. V. Kovalyov, F. I. Danilov. *Electrochim. Acta* **45**, 713 (1999).
26. P. C. Foller and W. Tobias. *J. Phys. Chem.* **85**, 3238 (1981).
27. P. C. Foller and G. H. Kelsall. *J. Appl. Electrochem.* **23**, 996 (1993).
28. Y. Beaufils, P. Bowen, C. Wenzed, Ch. Comminellis. *Proc.-Electrochem. Soc.* 97 (1998).
29. R. Amadelli, A. De Battisti, D. V. Girenko, S. V. Kovalyov, A. B. Velichenko. *Electrochim. Acta* **46**, 341 (2000).
30. W. Setz. *Pharm. Ind.* **47**, 15 (1985).
31. J. C. K. Ho, G. Tremiliosi Filho, R. Simpraga, B. E. Conway. *J. Electroanal. Chem.* **366**, 147 (1994).
32. O. Leitzke. *Internationales Symposium Ozon und Wasser*, Berlin, p. 164 (1977).
33. L. M. Da Silva, L. A. De Faria, J. F. C. Boodts. *Electrochim. Acta.* **47**, 395 (2001).
34. J. Feng and D. C. Johnson. *J. Electrochem. Soc.* **138**, 3328 (1991).
35. H. Chang and D. C. Johnson. *J. Electrochem. Soc.* **136**, 17 (1989).
36. D. W. Wabner and C. Grambow. *J. Electroanal. Chem.* **195**, 95 (1985).
37. D. M. Shub and M. F. Reznik. *Elektrokhimiya* **21**, 855 (1985).
38. L. M. Da Silva, J. F. C. Boodts, L. A. De Faria. *Electrochim. Acta* **46**, 1369 (2001).
39. L. A. da Silva, V. A. Alves, M. A. P. da Silva, S. Trasatti, J. F. C. Boodts. *Can. J. Chem.* **75**, 1483 (1997).
40. L. A. De Faria, J. F. C. Boodts, S. Trasatti. *J. Appl. Electrochem.* **26**, 1195 (1996).
41. C. N. Ho and B. J. Hwang. *J. Electroanal. Chem.* **377**, 177 (1994).
42. B. E. Conway, D. J. Mackinnon, B. V. Tilak. *Trans. Faraday Soc.* **66**, 1203 (1970).
43. P. Rüetschi. *J. Electrochem. Soc.* **106**, 819 (1959).
44. C. G. Jordanis, H. P. Fritz, D. Wabner. *J. Appl. Electrochem.* **14**, 389 (1984).
45. W. Smith and J. G. Hoogland. *Electrochim. Acta* **16**, 981 (1971).
46. K. Fukuda, C. Iwakura, H. Tamura. *Electrochim. Acta* **23**, 613 (1978).
47. I. Scheler and D. W. Wabner. *Z. Naturforsch.* **45b**, 892 (1990).
48. A. Hickling and S. Hill. *Trans. Faraday Soc.* **40**, 550 (1950).